

# Event-Free Moving Object Segmentation from Moving Ego Vehicle

Zhuyun Zhou<sup>1\*</sup> Zongwei Wu<sup>2\*</sup> Danda Pani Paudel<sup>3,4</sup> Rémi Boutteau<sup>5</sup> Fan Yang<sup>6</sup>  
 Luc Van Gool<sup>3,4</sup> Radu Timofte<sup>2</sup> Dominique Ginjac<sup>1</sup>

<sup>1</sup> ICB, UMR CNRS 6303, University of Burgundy <sup>2</sup> Computer Vision Lab, University of Würzburg <sup>3</sup> CVL, ETH Zurich

<sup>4</sup> INSAIT, Sofia University <sup>5</sup> LITIS, UR 4108, University of Normandy <sup>6</sup> LEAD, UMR CNRS 5022, University of Burgundy

## Abstract

Moving object segmentation (MOS) in dynamic scenes is challenging for autonomous driving, especially for sequences obtained from moving ego vehicles. Most state-of-the-art methods leverage motion cues obtained from optical flow maps. However, since these methods are often based on optical flows that are pre-computed from successive RGB frames, this neglects the temporal consideration of events occurring within inter-frame and limits the practicality of these methods in real-life situations. To address these limitations, we propose to exploit event cameras for better video understanding, which provide rich motion cues without relying on optical flow. To foster research in this area, we first introduce a novel large-scale dataset called DSEC-MOS for moving object segmentation from moving ego vehicles. Subsequently, we devise EmoFormer, a novel network able to exploit the event data. For this purpose, we fuse the event prior with spatial semantic maps to distinguish moving objects from the static background, adding another level of dense supervision around our object of interest - moving ones. Our proposed network relies only on event data for training but does not require event input during inference, making it directly comparable to frame-only methods in terms of efficiency and more widely usable in many application cases. An exhaustive comparison with 8 state-of-the-art video object segmentation methods highlights a significant performance improvement of our method over all other methods. Project Page: <https://github.com/ZZY-Zhou/DSEC-MOS>.

## 1. Introduction

Achieving precise moving object segmentations (MOS) in urban scenes plays a vital role in many vision tasks like image/video synthesis [46, 54]. This segmentation is always achieved through cross-frame affinity matrices [21, 57]. However, in more challenging scenarios, such

\*equal contribution.

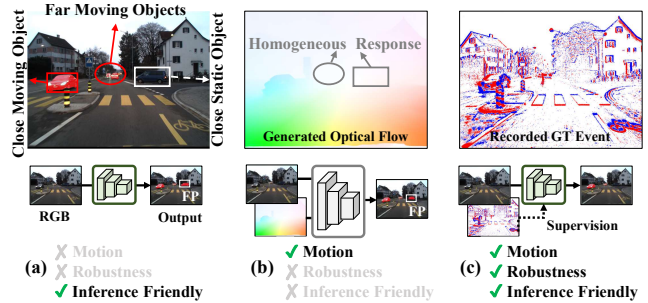


Figure 1. **Motivation.** (a) Segmenting moving objects from moving vehicles is challenging [19], which may lead to false positive (FP) results. (b) SOTA flow-based VOS method [63] also performs poorly, mainly due to the low-quality flow input [47] in the presence of ego motion. (c) We achieve more accurate prediction by leveraging event prior during training, while being event-free during inference. Please zoom in for details.

as videos recorded from moving ego vehicles, conventional methods often falter, as shown in Figure 1(a), primarily due to the significant impact of unavoidable ego-motion [23, 33]. Consequently, there exists a critical need for a high-performing MOS model from moving ego vehicles.

In the search for more robust and adaptive solutions, numerous previous works have attempted to incorporate additional motion cues, especially from the optical flow [17, 42, 47], to augment appearance-based features with improved temporal awareness [6, 62]. However, in some cases, only low-quality optical flow is available, especially in scenes with unclear object boundaries [58] due to scene depth or illumination conditions, as shown in Figure 1(b). Moreover, since the optical flow is usually computed from two consecutive frames [16, 47], the rapid motion that occurs in high dynamic scenes within a short time interval can be unfortunately neglected.

Recently, event cameras [11, 13] have disrupted traditional computer vision paradigms. Different from frame-based cameras, event cameras operate asynchronously [11], enabling them to capture rapid motion and react to dynamic scenes with remarkable precision. In addition, their sensitivity to pixel intensity changes and innate ability to adapt to

varying illumination conditions make them a robust choice for challenging scenarios [5, 27].

In this work, we aim to fully exploit the potential of event cameras for MOS from moving ego vehicles. Our problem differs from conventional (automatic) video object segmentation (VOS) [69] in three crucial aspects: (a) VOS typically aims to segment salient or foreground objects [15, 31], often a single object, while our goal is to segment all moving objects at once; (b) most automatic VOS methods preprocess the optical flow as input [8, 65] while we leverage ground truth event data; (c) in VOS, the camera motion is usually negligible compared to the object motion, while in our scenarios both objects and the cameras (embedded in the ego vehicle) are in unknown motion. These differences make our task an exceptional challenge, which, to our knowledge, is the first time being addressed comprehensively.

In our pursuit of robustly distinguishing between moving and static objects in dynamic scenes, we leverage the event prior to improve the motion pattern modeling. Our motivation comes from the observation that event data, by its nature, captures fine-grained details at the pixel level. Moreover, where events unfold, the most informative distribution centers around object motions, showcasing a strong correlation with the precise spatial boundaries of these objects, as shown in Figure 1(c). However, a significant challenge emerges due to the ego vehicle’s motion, complicating the differentiation between static and truly moving objects based solely on scene motion. To address this challenge, we propose to integrate event data with ground truth semantic masks. The “true” fine-grained event representation serves as a form of dense supervision for the model, providing it with a pixel-level insight into the occurrences of moving objects. This level of granularity allows the network to discern the subtlest of details, constraining the model’s attention around the intricate dynamics of moving objects. While the motivation for using event data is similar to previous works [28, 50, 72], our method stands out as the first to explicitly bridge the gap between event-based dense supervision and semantic clues.

To promote the research in the domain, we introduce a substantial dataset of 13,314 frames, derived from the DSEC dataset [12, 72]. This new dataset, called DSEC-MOS, covers a wide range of challenging driving scenarios, including different lighting conditions and complex traffic scenarios. It includes 8 categories of moving objects such as vehicles, pedestrians, cyclists, etc., each with different motion patterns, appearances, and scales, making the dataset highly suitable for both training and evaluation of MOS algorithms. Furthermore, DSEC-MOS provides dense pixel-level annotations for moving objects.

Leveraging our proposed dataset, we performed a systematic benchmark involving 8 state-of-the-art RGB and RGB-flow methods. Intriguingly, we observe that the lead-

ing methods [8, 19, 31, 63] on existing VOS datasets do not necessarily maintain their competitiveness on our challenging dataset. Nevertheless, with the same backbone, RGB-flow methods [31, 63] consistently outperform RGB-only approaches [8, 24]. Additionally, [19, 31] with deeper architectures such as transformers [52] outperform CNN-based counterparts [37, 59] even when the latter uses extra flow cues. Consequently, we introduce a straightforward yet highly effective model, termed EmoFormer, that incorporates event clues as additional dense supervision during training while remaining event-free during inference.

Detailed comparative analyses show that our method significantly outperforms all existing SOTA VOS approaches.

In summary, our contributions are two-fold:

- We introduce a new MOS task with moving ego vehicles and present a generously sized and densely annotated dataset called DSEC-MOS. We rigorously benchmark 8 SOTA video object segmentation methods to facilitate further work in this field.
- We introduce EmoFormer, which fully benefits from event clues during training while being event-free during inference. Our model outperforms all SOTA counterparts by a large margin.

## 2. Related Work

**Automatic Video Object Segmentation (AVOS):** AVOS represents a specialized task focused on segmenting objects within video sequences without prior knowledge about the target objects [69]. Within the realm of AVOS, the primary cues for segmentation stem from the motion exhibited by objects. Traditional approaches involve computing similarity matrices [43, 53, 61] across different video frames, implicitly harnessing temporal context to guide object identification. Another category of AVOS methods [7, 41, 60, 68, 71] explicitly uses the optical flow as a guiding cue. Considering that target objects in AVOS are typically salient and predominantly occupy the foreground, and camera motion is generally negligible in comparison to object motion [4, 32, 35], extracting the target object from the flow map is relatively straightforward compared to a real-world setting [9]. By combining appearance and motion cues, these methods tend to outperform RGB-baseline methods. However, one drawback is the need for flow map pre-processing, which can be impractical for applications like autonomous driving.

**Motion Segmentation:** Exhibiting certain parallels with AVOS, motion segmentation concentrates on discovering moving objects. Some approaches [40, 56] focus on pixel clustering based on similar motion patterns. Alternatively, [48, 49] delve into training deep networks to establish mappings from motions to segmentation masks. In [3, 22], the proposed methodology involves highlighting independently moving objects through compensation for background mo-

tion, achieved either by registering consecutive frames or explicitly estimating camera motion. In specific applications, such as autonomous driving scenarios, [36] advocates for a holistic optimization encompassing depth, camera motion, optical flow, and motion segmentation.

**Event Vision and Benchmarking:** Event cameras have attracted considerable research interest due to their unique ability to capture rapid motion through asynchronous event processing [2, 34, 38, 74]. Recent studies [1, 10, 45] have begun to explore the potential of event data for high-level tasks, especially in the context of driving scenarios. Pioneering works, such as [12, 73], have collected large RGB-Event datasets tailored to urban scenes. Nevertheless, these datasets often lack comprehensive manual high-level annotations. Some approaches resort to off-the-shelf techniques to generate pseudo ground truth annotations, such as the use of YOLO bounding boxes [50] or semantic segmentation [44]. However, the quality of such pseudo annotations may be limited. Furthermore, these efforts typically focus on global detection without distinguishing between motion features, *i.e.*, discerning moving objects from static ones. The concurrent works [29, 66, 70] detect moving objects but only a small number of sequences with indoor event input. In this paper, we introduce a novel large-scale MOS dataset that provides pixel-level annotations of scenes with moving ego vehicles. Our dataset stands as the first of its kind, designed specifically to tackle the distinctive challenges posed by moving objects in dynamic urban environments.

### 3. Methodology

#### 3.1. Preliminaries of Video Segmentation

**Frame-based Methods:** We initiate this section with an architectural overview of frame-based video segmentation. Given a video clip, denoted as  $\{I_t \in \mathbb{R}^{3 \times H \times W}\}_{t=1}^T$ , comprising a sequence of  $T$  frames, the objective of video segmentation is to predict masks  $\{P_t \in \mathbb{R}^{H \times W}\}_{t=1}^T$  corresponding to the moving objects within the frames. These predicted masks are intended to closely align with the ground truth masks  $\{M_t \in \mathbb{R}^{H \times W}\}_{t=1}^T$  for the respective frames. For the sake of brevity in subsequent discussions, we employ the notation  $\{.\}$  to represent the set  $\{.\}_{t=1}^T$ .

In the field of conventional RGB-based models [19, 24, 26, 53, 67],

the extraction of multi-scale features is a common practice, which is usually achieved by  $L$  intermediate layers within the deep encoder. Subsequently, various learning modules are employed to construct an affinity matrix that encompasses both temporal frames and spatial scales to capture spatio-temporal awareness. Finally, the decoder phase is responsible for projecting the refined features onto semantic logits.

Herein, we denote the encoder, the affinity modeling,

the decoder, and the loss function as  $\mathcal{E}(\cdot)$ ,  $\mathcal{A}(\cdot)$ ,  $\mathcal{D}(\cdot)$ , and  $\mathcal{L}_{sem}(\cdot)$ , respectively. The overall learning pipeline can be succinctly summarized as follows:

$$\begin{aligned} \{P_t\} &= \mathcal{D}(\mathcal{A}(\mathcal{E}(\{I_t\}))); \\ \text{argmin } \mathcal{L}_{sem}(\{P_t\}; \{M_t\}). \end{aligned} \quad (1)$$

**RGB-Flow Methods:** Although frame-based methods have provided satisfactory results, the implicit learning approach, which incorporates the motion/affinity matrix across frames, has certain limitations. As a result, numerous models [8, 31, 37, 59, 63] have adopted a dual-stream learning pipeline that integrates both RGB and optical flow data as inputs, where the optical flow  $\{O_t \in \mathbb{R}^{3 \times H \times W}\}$  is typically pre-computed using a pre-trained and frozen weight estimation network. Instead of directly learning the affinity matrix, these approaches introduce fusion modules that aim to harmonize appearance and motion cues within the latent feature space. Let  $\mathcal{E}_1(\cdot)$ ,  $\mathcal{E}_2(\cdot)$ ,  $\mathcal{F}(\cdot)$ ,  $\mathcal{D}(\cdot)$ , and  $\mathcal{L}_{sem}(\cdot)$  be the RGB encoder, the flow encoder, the fusion module, the decoder, and the loss function, respectively. The holistic learning pipeline is then:

$$\begin{aligned} \{P_t\} &= \mathcal{D}(\mathcal{F}(\mathcal{E}_1(\{I_t\}); \mathcal{E}_2(\{O_t\}))); \\ \text{argmin } \mathcal{L}_{sem}(\{P_t\}; \{M_t\}). \end{aligned} \quad (2)$$

**Limitations:** While flow-based methods generally perform better compared to RGB baseline, the need for optical flow as input poses a practical challenge for real-world applications. Furthermore, while RGB-flow fusion modules can enhance temporal consistency, they often fail to effectively capture spatial cues, which are also critical for object segmentation. Finally, as mentioned earlier, pre-computed optical flow inherently carries several limitations that make it suboptimal for MOS.

In the following sections, we introduce our end-to-end learnable EmoFormer as shown in Figure 2. In contrast to the conventional approach of pre-computing the optical flow, our method harnesses motion cues directly from the recorded event data. Moreover, we seamlessly integrate the event prior into our spatio-temporal supervision scheme, resulting in event-free inference. This pivotal advance not only brings our model on par with RGB networks but also improves its suitability for real-world applications.

#### 3.2. Prior Generation

Without loss of generalizability, we take the encoded RGB feature  $F_{rgb} \in \mathbb{R}^{c \times h \times w}$  from the last layer of the backbone from one image as an example. While the RGB feature is rich in appearance information, it inherently lacks awareness of temporal variations. Although inner-frame motion can be modeled by comparing two consecutive images, the video’s limited frames per second (FPS) restrict its ability to capture rapid motion. Hence, our objective is to

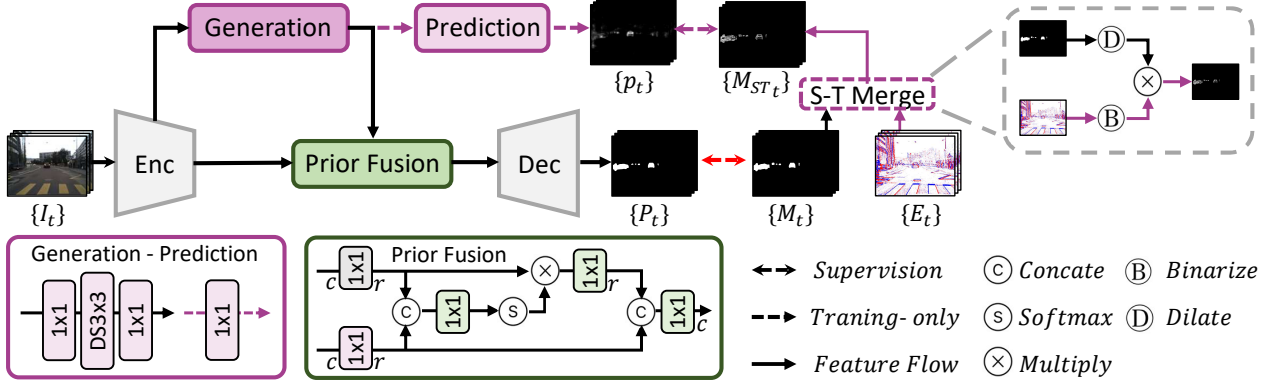


Figure 2. **Architecture.** In addition to the standard RGB Encoder-Decoder architecture, we introduce an auxiliary branch dedicated to harnessing the motion insights derived from the recorded event data (Section 3.2). This learned representation is subsequently merged into the main processing pipeline, thereby enhancing feature modeling (Section 3.3). To further refine event-based learning and the understanding of object dynamics, we employ semantic maps to transfer global scene motion into targeting objects’ motion (Section 3.4). Such a merging strategy leads to a tightly coupled Spatio-Temporal awareness, ultimately shaping our joint learning scheme.

estimate the rapid motion from a single RGB image, with the help of event data acquired during the frame time.

Specifically, we use a combination of (depth-separated) convolutions as the generation module. First, we project  $F_{rgb}$  into a deeper latent feature space using a  $Conv_{1 \times 1}$  operation, capture local motion awareness with  $DSConv_{3 \times 3}$ , and then project the result back using another  $Conv_{1 \times 1}$ . The choice of depth-separate convolution stems from the observation that rapid motion typically occurs within a localized region, as illustrated in Figure 1. Furthermore, the depth-wise convolution contributes to efficient processing. Consequently, we obtain an intermediate representation corresponding to the high dynamic features, denoted as  $F_m \in \mathbb{R}^{c \times h \times w}$ . Mathematically, we have:

$$F_m = Conv_{1 \times 1}(DSConv_{3 \times 3}(Conv_{1 \times 1}(F_{rgb}))). \quad (3)$$

To provide explicit guidance for the intermediate feature, we initially use a  $Conv_{1 \times 1}$  operation to generate a one-channel prediction map  $p_m$  based on  $F_m$ . We then integrate event supervision, as described in Section 3.4.

### 3.3. Prior Fusion

To seamlessly integrate the high dynamic feature  $F_m$  with the visual feature  $F_{rgb}$ , we introduce a novel prior fusion framework shown in Figure 2. Traditional RGB-Event fusion methods such as [50] often operate in an equal or higher dimensional feature space. However, the direct application of such methods to our context poses a challenge. Since one feature is estimated based on the other, even with event supervision, it may still exhibit a high degree of redundancy compared to the other. Consequently, these methods may retain redundant information rather than mutually complementary ones.

In contrast, following recent developments such as LoRA [14], we propose to project both of these features into

a smaller subspace, denoted as  $r \ll C$ . This projection can be likened to a low-rank decomposition, wherein only the most informative modality-specific features are preserved. Moreover, this approach naturally reduces the computational overhead compared to alternative fusion techniques. Mathematically, we achieve this projection as follows:

$$f_{rgb} = Conv_{1 \times 1}(F_{rgb}); \quad f_m = Conv_{1 \times 1}(F_m). \quad (4)$$

We then conduct cross-modal feature modeling within this lower-dimensional space  $r$ . Given the inherent domain gap between visual and motion cues, our objective is to identify a shared embedding on which effective fusion can occur. To facilitate this, we initially concatenate these feature maps, forming a correlation matrix  $f_c \in \mathbb{R}^{r \times h \times w}$ . From this matrix, we derive per-pixel attention weights using a global Softmax function:

$$Att = Softmax(f_c); \quad (5)$$

$$f_c = Conv_{1 \times 1}(Concat(f_{rgb}; f_m)).$$

We then apply this attention map to the low-rank RGB feature, thereby mitigating the domain gap. Finally, we obtain the shared embedding by merging the attention-enhanced RGB feature and the motion feature by concatenation. Finally, this mixed embedding is projected back into the full-rank space  $C$  to yield the fused feature  $F_u \in \mathbb{R}^{c \times h \times w}$ . We have:

$$F_s = Conv_{1 \times 1}(Concat(f_{rgb} \times Att; f_m)). \quad (6)$$

### 3.4. Spatio-Temporal Dense Supervision

Event data provide invaluable insights into the global scene motion. However, the dense distribution of events is not solely limited to areas occupied by moving objects, but

can also encompass the contours of static or background elements. This complexity arises from the fact that our ego vehicle is also in motion, which makes it difficult to discern the motion exclusively associated with the target objects.

To solve this dilemma, we propose a novel approach that combines event data with ground truth semantic supervision. This hybrid strategy allows us to pass from the overall scene motion into the object motion, constraining the network attention around the moving object with dense supervision at pixels.

Specifically, it involves suppressing background regions by element-wise multiplication with the spatial semantic mask. However, the direct multiplication of the spatial semantic mask with the temporal event map can inadvertently remove essential motion cues, especially when the event motion map extends beyond the object boundaries due to motion blur. To mitigate this, we employ a dilation operation on the spatial mask with a specified kernel size before conducting spatio-temporal fusion. Mathematically, let  $M \in \mathbb{R}^{H \times W}$  be the ground truth (GT) semantic mask,  $D \in \mathbb{R}^{3 \times 3}$  be the dilation matrix, and  $E \in \mathbb{R}^{H \times W}$  be the event data. The spatio-temporal map  $M_{ST} \in \mathbb{R}^{H \times W}$  is obtained by:

$$M_{ST} = (M \oplus D) \circ E, \quad (7)$$

where  $\oplus$  is the morphological dilation and  $\circ$  is the Hadamard product. In our application, we set  $D$  as an all-ones matrix, and we treat positive and negative polarization changes equally in the binary form of event data.

Subsequently, we utilize  $M_{ST}$  to supervise the intermediate representation  $p_m$  introduced in Section 3.2. To minimize the disparity between these two maps, we leverage conventional MSE loss as the auxiliary loss denoted as  $\mathcal{L}_{ST}$ .

### 3.5. Overall Learning Pipeline

Our event-guided training methodology departs from the conventional RGB learning pipeline by introducing additional spatio-temporal supervision. We denote the conventional components as  $\mathcal{E}(\cdot)$ ,  $\mathcal{D}(\cdot)$ , and  $\mathcal{L}_{sem}(\cdot)$ , mirroring the RGB learning pipeline. For more details, we refer readers to [19] for the RGB baseline we used. In addition to these components, we incorporate the extra prior generation module (Section 3.2) and the prior fusion module (Section 3.3), represented as  $\mathcal{G}(\cdot)$  and  $\mathcal{F}(\cdot)$ , respectively. We introduce  $\mathcal{P}(\cdot)$  as a convolution-based prediction. The overall learning pipeline can be summarized as follows:

$$\begin{aligned} \{F_t\} &= \mathcal{E}(\{I_t\}); & \{F_{m_t}\} &= \mathcal{G}(\{F_t\}); \\ \{p_{m_t}\} &= \mathcal{P}(\{F_{m_t}\}); & \{P_t\} &= \mathcal{D}(\mathcal{F}(\{F_t\}; \{F_{m_t}\})); \\ \text{argmin} & [\mathcal{L}_{sem}(\{P_t\}; \{M_t\}) + \mathcal{L}_{ST}(\{p_{m_t}\}; \{M_{ST_t}\})]. \end{aligned} \quad (8)$$

It is noteworthy that the prediction  $\mathcal{P}(\cdot)$  is exclusively employed during training to leverage event supervision, but it

Table 1. DSEC-MOS Dataset Specification

	Frames / Masks	Training	Testing
Total	13,314 / 62,291	10,495 / 51,489	2,819 / 10,802
Day	7,188 / 34,058	5,923 / 29,463	1,265 / 4,595
Twilight	4,946 / 22,415	3,757 / 18,201	1,189 / 4,214
Night	1,180 / 5,818	815 / 3,825	365 / 1,993

is not required during testing. During inference, our model operates solely on frames, ensuring an event-free process.

## 4. Our DSEC-MOS Dataset

### 4.1. Dataset Annotation

Our DSEC-MOS dataset builds upon the DSEC-MOD dataset [72], originally designed for moving object detection with bounding box annotations. To create DSEC-MOS, we followed a systematic process:

**Candidate Mask Generation:** We initiated the process by employing the modified SOTA segmentation model [20] with bounding box prompts to generate candidate masks.

**Annotator Training:** Next, we train three annotators to become proficient in video segmentation tasks. They are provided with guidance and instructions on well-established VOS benchmarks to familiarize themselves with the task.

**Manual Verification:** After training, each annotator was tasked with reviewing the candidate masks, aided by reference to adjacent frames. If a candidate mask was found to be suboptimal with an incomplete shape or inaccurate detection, the annotator was asked to correct manually.

**Specialization by Illumination Condition:** Since our dataset comprises sequences captured under various illumination conditions, we assigned each annotator to sequences from one typical condition to develop specializations.

**Cross and Double Verification:** The sequences from each illumination condition underwent cross and double verification. In case of uncertainty or discrepancies, annotators were encouraged to discuss and jointly modify the masks until a consensus was reached.

### 4.2. Dataset Specification

**Dataset Size and Annotations:** As shown in Table 1, our dataset contains a total of 62,291 annotation masks and thus represents an extensive resource for the task. Notably, the well-known DAVIS-17 dataset [35] provides 13,541 annotated masks, while our dataset is about 5 times larger.

**Multi-modal Data:** For each sequence, we offer both recorded event data and optical flow (using RAFT [47]) in addition to the RGB frames. These features are synchronized with the RGB frames, making it possible to have a detailed analysis of per-frame motion for both flow and event.

**Object Variety:** The dataset includes a wide range of short-term and long-term sequences, featuring 8 distinct object



Figure 3. **DSEC-MOS examples.** From left to right: (a) Calibrated-to-Event RGB frames; (b) Our DSEC-MOS Ground Truth Segmentation Masks; (c) Ground Truth Masks visualized on calibrated RGB frames. Best zoomed in.

classes, namely cars, trucks, buses, trains, pedestrians, cyclists, motorcyclists, and others. These objects exhibit varying appearances, motions, and interactions over time, which poses a significant challenge for segmentation tasks. In particular, the SOTA video segmentation methods [31, 63] achieve about 90%  $\mathcal{J}\&\mathcal{F}$  on DAVIS-16 [32], whereas their performance is reduced to about 65% in our dataset.

**Real-World Scenarios:** DSEC-MOS encompasses a large variety of real-world driving scenarios, including different illumination conditions (day, twilight, night scenes) and varying traffic densities, and is therefore ideally suited for benchmarking MOS methods. Figure 3 provides some examples of our DSEC-MOS dataset, from which we visualize accurate fine-grained segmentation masks.

### 4.3. Dataset Comparison

In Table 2, we offer a comprehensive per-attribute comparison with established event-based segmentation datasets. Significantly, our dataset emerges as a pioneering initiative, distinguished as the first of its kind to provide dense MOS masks from a moving ego vehicle. While EV-IMO [29] stands as another notable MOS dataset, it is confined to indoor settings and lacks paired RGB frames. This absence hinders its applicability for assessing RGB models, underscoring the unique nature of our dataset.

We also show in Figure 4 the visual comparison with the DSEC Night-Sem dataset [55] which is the most closely related to ours. It’s important to highlight that our dataset outshines in terms of continuous labeling for all frames, offering a comprehensive view compared to the sporadic annotations as in [55]. Furthermore, our dataset explicitly distinguishes objects based on different motion types, a distinctive feature not addressed in Figure 4, adding a layer of complexity and uniqueness to our dataset.

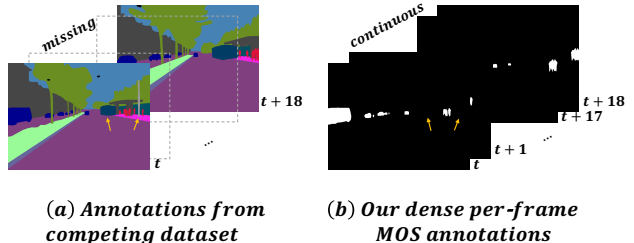


Figure 4. Dataset Visual Comparison. Our dataset provides per-frame annotation and distinguish the motion attribute, which are not available in the previous dataset [55].

Table 2. Datasets Per-Attribute Comparison.

Dataset	GT	Outdoor	Per-Frame	MOS
EV-IMO [29]	✓	✗	-	✓
DSEC-Sem [44]	✗	✓	✓	✗
DSEC Night-Sem [55]	✓	✓	✗	✗
<b>Ours</b>	✓	✓	✓	✓

## 5. Experiments

### 5.1. Experimental Setup

**Implementation Details:** We take video-swin [25] as the encoder that extracts features from 6 frames. Each input frame is resized to 360×409. Following [72], we leverage event data from 50ms, in accordance with the frame time. Classic data augmentation methods such as multi-scale training and flipping are adopted. We adopt AdamW as the optimizer, with an initial learning rate 1e-6 and 1e-4 for the backbone and others, respectively. The weight decay is set to 1e-4 and the polynomial learning rate decay is employed with a power of 0.9. Our network is built upon PyTorch. The whole network training takes around 3 days on a V100 GPU. Unlike most VOS works, our method does not require any pretraining on large-scale datasets. For benchmarking, we retrain all the SOTA counterparts from their official resources. For practical application consideration, we exclude the time-burden CRF post-processing for all.

**Evaluation Metrics:** We use classical evaluation metrics, including region similarity  $\mathcal{J}$  and contour accuracy  $\mathcal{F}$ , in accordance with the VOS tasks [32]. We compute both the mean and recall forms for each metric, as well as the overall performance  $\mathcal{J}\&\mathcal{F}$  based on the mean ones [9].

### 5.2. Benchmark and Comparison

It is noteworthy that our benchmark does not include comparisons with RGB-Event object segmentation methods, as none have been identified thus far. Despite the availability of certain semantic segmentation techniques [18, 44, 55, 64], these methods do not deal with the distinction between moving and static objects, so they do not fall within the scope of our benchmark.

**Comparison against SOTA Methods:** Our moving object

Table 3. **Quantitative Comparison** with SOTA AVOS Approaches on Our DSEC-MOS. Our EmoFormer outperforms both RGB and RGB-Flow counterparts with large margins. MS Inf. refers to Multi-Scale Inference. Our EmoFormer achieves the best performances during both single-scale and multi-scale inferences.

Method	Pub. & Year	Backbone	Optical Flow	MS Inf.	$\mathcal{J}$ Mean	$\mathcal{J}$ Recall	$\mathcal{F}$ Mean	$\mathcal{F}$ Recall	$\mathcal{J} \& \mathcal{F}$
RTNet [37]	CVPR'21	ResNet-101	✓	-	57.8	65.8	71.7	82.2	64.8
AMCNet [59]	ICCV'21	ResNet-101	✓	-	60.6	71.3	76.1	86.8	68.4
TMO [8]	WACV'23	ResNet-101	✓	-	56.2	62.1	73.0	82.8	64.6
Isomer [63]	ICCV'23	Swin-T	✓	-	55.9	65.3	72.2	86.0	64.1
F2Net [24]	AAAI'21	ResNet-50	-	-	45.1	48.4	66.9	74.5	56.0
TMO [8]	WACV'23	ResNet-101	-	-	53.5	57.1	70.3	81.8	61.9
MED-VT [19]	CVPR'23	Swin-B	-	-	58.0	67.3	81.0	90.6	69.5
<b>EmoFormer</b>	<b>Ours</b>	Swin-B	-	-	<b>61.6</b>	<b>73.0</b>	<b>82.2</b>	<b>92.5</b>	<b>71.9</b>
HFAN [31]	ECCV'22	Swin-T	✓	✓	62.6	69.5	76.8	85.7	69.7
MED-VT [19]	CVPR'23	Swin-B	✓	✓	63.5	71.8	81.5	90.3	72.5
<b>EmoFormer</b>	<b>Ours</b>	Swin-B	-	✓	<b>68.9</b>	<b>79.6</b>	<b>83.7</b>	<b>93.4</b>	<b>76.3</b>

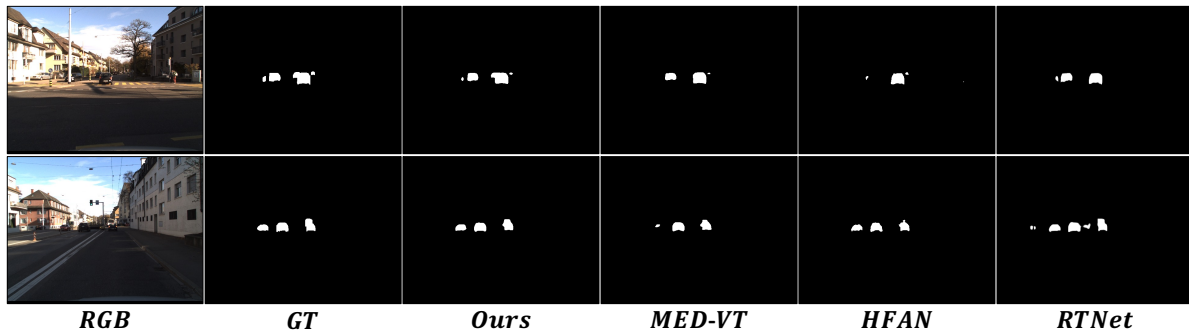


Figure 5. **Qualitative Comparison.** Our generated masks are closer to the ground truth. Best zoomed in.

segmentation task is very similar to automatic Video Object Segmentation (AVOS) tasks; in that we do not provide manual clues such as initial masks or bounding boxes to identify the target objects. Instead, we aim to automatically segment moving objects based solely on video sequences. To evaluate the effectiveness of our method, we compared 8 state-of-the-art automatic VOS methods as reported in Table 3. To ensure fair comparisons, we evaluated our performance with both single-scale and multi-scale inference techniques. The results demonstrate a significant performance improvement over all other methods. In the case of single-scale inference, our network significantly improves the performance of our RGB baseline (MED-VT) with an absolute gain of +3.6%  $\mathcal{J}$  Mean, outperforming the current state-of-the-art method, AMCNet [59]. It is worth noting that AMCNet requires both RGB and flow maps during inference, whereas our method operates only on RGB frames. In the case of multi-scale inference, we achieve an absolute gain of +5.4%  $\mathcal{J}$  Mean over MED-VT. We also provide qualitative comparisons in Figure 5, illustrating that our method excels at exploring temporal cues and generating prediction masks that closely match ground truth, outperforming any pure RGB or RGB-Flow counterparts. More visualizations can be found in the accompanying video.

**Comparison under different illumination conditions:** In

Table 4. Comparison of performance between baseline and our EmoFormer according to illumination variance.

Illum.	Comp.	$\mathcal{J}$ Mean	$\mathcal{F}$ Mean	$\mathcal{J} \& \mathcal{F}$
Overall	RGB	63.5	81.5	72.5
	<b>+ Ours</b>	<b>68.9 (+5.4)</b>	<b>83.7 (+2.2)</b>	<b>76.3 (+3.8)</b>
Day	RGB	71.0	85.9	78.5
	<b>+ Ours</b>	<b>76.5 (+5.5)</b>	<b>87.8 (+1.9)</b>	<b>82.2 (+3.7)</b>
Twilight	RGB	57.3	78.4	67.9
	<b>+ Ours</b>	<b>59.8 (+2.5)</b>	<b>78.6 (+0.2)</b>	<b>69.2 (+1.3)</b>
Night	RGB	47.2	71.3	59.3
	<b>+ Ours</b>	<b>55.4 (+8.2)</b>	<b>76.3 (+5.0)</b>	<b>65.9 (+6.6)</b>

this work, we seek to gain deeper insights into the impact of event cameras by conducting a thorough performance analysis across varying illumination scenarios. Detailed findings of this comparative assessment are presented in Table 4, showcasing the effectiveness of complementary events. Notably, our modules exhibit remarkable and consistent improvement over baseline across all conditions.

### 5.3. Ablation Studies

We perform multi-scale inference for ablation studies. **Supervision Strategies:** In our training pipeline, we leverage event data as auxiliary supervision, facilitated by a semantic mask. To assess the effectiveness of this approach, we conducted experiments in which we replaced the intermediate representation with alternative supervision meth-

Table 5. **Ablation Study on Supervision Strategies.**  $\circ$  is the Hadamard multiplication to suppress static responses.

Aux. Sup. Source	$\circ$ GT	Dilation	$\mathcal{J}$ M	$\mathcal{F}$ M	$\mathcal{J}$ & $\mathcal{F}$
1	-	-	63.5	81.5	72.5
2	Flow	-	66.2	80.7	73.5
3	Semantic	-	67.2	82.2	74.7
4	Semantic	✓	67.6	83.1	75.4
5	Event	-	65.4	80.1	72.8
6	Event	✓	67.9	82.8	75.4
7	Event	✓	<b>68.9</b>	<b>83.7</b>	<b>76.3</b>

Table 6. **Ablation study on Fusion Alternatives.**

#	Fusion	$\mathcal{J}$ Mean	$\mathcal{F}$ Mean	$\mathcal{J}$ & $\mathcal{F}$
1	-	63.5	81.5	72.5
2	Addition	66.5	82.1	74.3
3	Multiplication	65.2	82.3	73.8
4	FPN-Fusion [50]	67.7	82.3	75.0
5	Ours	<b>68.9</b>	<b>83.7</b>	<b>76.3</b>

ods, such as optical flow only, semantic mask only, and event data only. The quantitative results are shown in Table 5. It is evident that, while the auxiliary supervisions consistently improve our baseline, their individual performance is inferior to our full approach. We observed that omitting the semantic map guidance and the dilation operation leads to performance deterioration. This outcome can be attributed to the role of semantic guidance in attenuating noisy event responses from static regions. In addition, dilation plays a crucial role in the alignment of spatial masks with temporal motion blur.

**Fusion choices:** We also conducted experiments to validate our fusion strategies. The results are reported in Table 6. Specifically, we replaced our fusion module with various alternatives, ranging from simple addition operations to tailored RGB-Event fusion modules [50]. Our superior performance confirms the effectiveness of our fusion approach.

#### 5.4. What Can Moving MOS Do?

The exploration of MOS from moving vehicles is still a relatively unexplored area compared to segmentation tasks in the field of autonomous driving. This gap is not only due to the scarcity of labeled data but also due to the inherent challenges that arise from the nuanced interplay between relatively static and truly moving objects, making the segmentation task even more complex. In this discussion, we will dive a little deeper into the dynamics of moving MOS using the insights from our dataset.

The primary goal is to delineate the difference between object motion and scene motion. This distinction can be incredibly subtle due to the relative static speed in dynamic scenes. We propose that this subtlety can be improved by leveraging true semantic clues — a concept that has been validated in previous works on motion magnification [30, 39] and object flow analysis [51]. This enhancement is

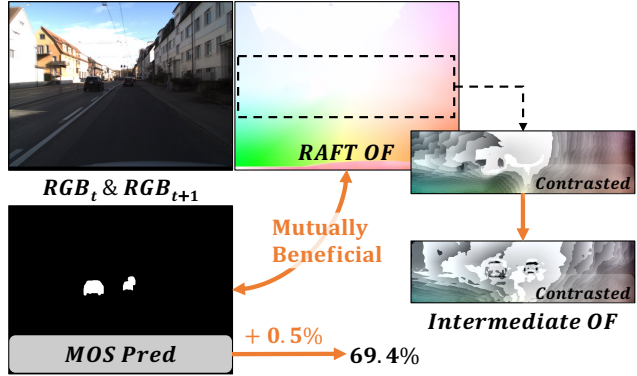


Figure 6. **MOS and Optical Flow.** We transfer the input flow into an intermediate representation, with the help of the semantic clues, leading to stronger activations around the relatively static but truly moving objects. This in turn improves the semantic prediction, with +0.5% on  $\mathcal{J}$  mean, showing the mutual benefits between MOS and flow. Best zoomed in.

expected to be mutually beneficial, as a refined understanding of motion should, in turn, increase semantic precision.

To confirm this hypothesis, we introduce an additional flow component, that works in parallel with our mask head. This mask head predicts optical flow — an intermediate representation supervised by RAFT estimation. Furthermore, it estimates a mask output by combining visual features, supervised by the ground truth masks. Detailed insights into the model design can be found in the supplementary material. As depicted in Figure 6, the conventional RAFT flow struggles to provide meaningful clues for relatively static but truly moving objects. Contrastingly, our estimated intermediate flow exhibits stronger activations around these objects of interest. This process, enhanced by semantic clues, elevates objects of interest above their neighboring pixels, overcoming the challenges posed by their distance from the ego vehicle and distracting surfaces. The natural result binary-like mask effectively bridges the gap between subtle motion nuances and semantics. Quantitatively, our approach achieves an extra absolute gain of +0.5% in  $\mathcal{J}$  Mean, elevating performance from 68.9% to 69.4%, validating our departing hypothesis.

## 6. Conclusion

We demonstrate the effectiveness of using the event prior for moving object segmentation in dynamic scenes. Our method combines the inherent advantages of event data for capturing global motion with semantic supervision. This leads to an intermediate representation that enables the network to separate moving objects from the static background, resulting in another level of dense supervision. Moreover, our method no longer requires any event input during inference, which makes it particularly efficient and suitable for real-world applications based on standard



RGB cameras. We also introduce a new large-scale dataset designed for moving object segmentation in dynamic autonomous driving scenarios, which is the first of its kind. Our method significantly outperforms the state of the art and confirms the potential of event-based pipelines for autonomous driving. To sum up, we hope that our method and dataset can promote further research in this field.

## References

- [1] Alexander Amini, Tsun-Hsuan Wang, Igor Gilitschenski, Wilko Schwarting, Zhijian Liu, Song Han, Sertac Karaman, and Daniela Rus. Vista 2.0: An open, data-driven simulator for multimodal sensing and policy learning for autonomous vehicles. In *ICRA*. IEEE, 2022. 3
- [2] R Wes Baldwin, Ruixu Liu, Mohammed Almatrafi, Vijayan Asari, and Keigo Hirakawa. Time-ordered recent event (tore) volumes for event cameras. *IEEE TPAMI*, 45(2):2519–2532, 2022. 3
- [3] Pia Bideau and Erik Learned-Miller. It’s moving! a probabilistic model for causal motion segmentation in moving camera videos. In *ECCV*. Springer, 2016. 2
- [4] Sergi Caelles, Alberto Montes, Kevis-Kokitsi Maninis, Yuhua Chen, Luc Van Gool, Federico Perazzi, and Jordi Pont-Tuset. The 2018 davis challenge on video object segmentation. *arXiv preprint arXiv:1803.00557*, 2018. 2
- [5] Guang Chen, Hu Cao, Jorg Conradt, Huajin Tang, Florian Rohrbein, and Alois Knoll. Event-based neuromorphic vision for autonomous driving: A paradigm shift for bio-inspired visual sensing and perception. *IEEE SPM*, 37(4): 34–49, 2020. 2
- [6] Jingchun Cheng, Yi-Hsuan Tsai, Shengjin Wang, and Ming-Hsuan Yang. Segflow: Joint learning for video object segmentation and optical flow. In *ICCV*, 2017. 1
- [7] MyeongAh Cho, Taeh Kim, Woo Jin Kim, Suhwan Cho, and Sangyoun Lee. Unsupervised video anomaly detection via normalizing flows with implicit latent features. *PR*, 129: 108703, 2022. 2
- [8] Suhwan Cho, Minhyeok Lee, Seunghoon Lee, Chaewon Park, Donghyeong Kim, and Sangyoun Lee. Treating motion as option to reduce motion dependency in unsupervised video object segmentation. In *WACV*, 2023. 2, 3, 7
- [9] Henghui Ding, Chang Liu, Shuting He, Xudong Jiang, Philip HS Torr, and Song Bai. Mose: A new dataset for video object segmentation in complex scenes. In *ICCV*, 2023. 2, 6
- [10] Ziluo Ding, Rui Zhao, Jiyuan Zhang, Tianxiao Gao, Ruiqin Xiong, Zhaofei Yu, and Tiejun Huang. Spatio-temporal recurrent networks for event-based optical flow estimation. In *AAAI*, 2022. 3
- [11] Guillermo Gallego, Tobi Delbrück, Garrick Orchard, Chiara Bartolozzi, Brian Taba, Andrea Censi, Stefan Leutenegger, Andrew J Davison, Jörg Conradt, Kostas Daniilidis, et al. Event-based vision: A survey. *IEEE TPAMI*, 44(1):154–180, 2020. 1
- [12] Mathias Gehrig, Willem Aarents, Daniel Gehrig, and Davide Scaramuzza. Dsec: A stereo event camera dataset for driving scenarios. *IEEE RAL*, 6(3):4947–4954, 2021. 2, 3
- [13] Shasha Guo and Tobi Delbruck. Low cost and latency event camera background activity denoising. *IEEE TPAMI*, 45(1): 785–795, 2022. 1
- [14] Edward J Hu, Yelong Shen, Phillip Wallis, Zeyuan Allen-Zhu, Yuanzhi Li, Shean Wang, Lu Wang, and Weizhu Chen. LoRA: Low-rank adaptation of large language models. In *ICLR*, 2022. 4
- [15] Yuan-Ting Hu, Jia-Bin Huang, and Alexander G Schwing. Unsupervised video object segmentation using motion saliency-guided spatio-temporal propagation. In *ECCV*, 2018. 2
- [16] Zhaoyang Huang, Xiaoyu Shi, Chao Zhang, Qiang Wang, Ka Chun Cheung, Hongwei Qin, Jifeng Dai, and Hongsheng Li. Flowformer: A transformer architecture for optical flow. In *ECCV*. Springer, 2022. 1
- [17] Eddy Ilg, Nikolaus Mayer, Tonmoy Saikia, Margret Keuper, Alexey Dosovitskiy, and Thomas Brox. FlowNet 2.0: Evolution of optical flow estimation with deep networks. In *CVPR*, 2017. 1
- [18] Zexi Jia, Kaichao You, Weihua He, Yang Tian, Yongxiang Feng, Yaoyuan Wang, Xu Jia, Yihang Lou, Jingyi Zhang, Guoqi Li, et al. Event-based semantic segmentation with posterior attention. *IEEE TIP*, 32:1829–1842, 2023. 6
- [19] Rezaul Karim, He Zhao, Richard P Wildes, and Mennatul-lah Siam. Med-vt: Multiscale encoder-decoder video transformer with application to object segmentation. In *CVPR*, 2023. 1, 2, 3, 5, 7
- [20] Alexander Kirillov, Eric Mintun, Nikhila Ravi, Hanzi Mao, Chloe Rolland, Laura Gustafson, Tete Xiao, Spencer Whitehead, Alexander C Berg, Wan-Yen Lo, et al. Segment anything. In *ICCV*, 2023. 5
- [21] Abhijit Kundu, Kyle Genova, Xiaoqi Yin, Alireza Fathi, Caroline Pantofaru, Leonidas J Guibas, Andrea Tagliasacchi, Frank Dellaert, and Thomas Funkhouser. Panoptic neural fields: A semantic object-aware neural scene representation. In *CVPR*, 2022. 1
- [22] Hala Lamdouar, Charig Yang, Weidi Xie, and Andrew Zisserman. Betrayed by motion: Camouflaged object discovery via motion segmentation. In *ACCV*, 2020. 2
- [23] Yingping Liang, Jiaming Liu, Debing Zhang, and Ying Fu. Mpi-flow: Learning realistic optical flow with multiplane images. In *ICCV*, 2023. 1
- [24] Daizong Liu, Dongdong Yu, Changhu Wang, and Pan Zhou. F2net: Learning to focus on the foreground for unsupervised video object segmentation. In *AAAI*, 2021. 2, 3, 7
- [25] Ze Liu, Jia Ning, Yue Cao, Yixuan Wei, Zheng Zhang, Stephen Lin, and Han Hu. Video swin transformer. In *CVPR*, 2022. 6
- [26] Xiankai Lu, Wenguan Wang, Chao Ma, Jianbing Shen, Ling Shao, and Fatih Porikli. See more, know more: Unsupervised video object segmentation with co-attention siamese networks. In *CVPR*, 2019. 3
- [27] Ana I Maqueda, Antonio Loquercio, Guillermo Gallego, Narciso García, and Davide Scaramuzza. Event-based vision meets deep learning on steering prediction for self-driving cars. In *CVPR*, 2018. 2

- [28] Nico Messikommer, Daniel Gehrig, Mathias Gehrig, and Davide Scaramuzza. Bridging the gap between events and frames through unsupervised domain adaptation. *IEEE RAL*, 7(2):3515–3522, 2022. 2
- [29] Anton Mitrokhin, Chengxi Ye, Cornelia Fermüller, Yiannis Aloimonos, and Tobi Delbruck. Ev-imo: Motion segmentation dataset and learning pipeline for event cameras. In *IROS*. IEEE, 2019. 3, 6
- [30] Tae-Hyun Oh, Ronnachai Jaroensri, Changil Kim, Mohamed Elgharib, Fr’edo Durand, William T Freeman, and Wojciech Matusik. Learning-based video motion magnification. In *ECCV*, 2018. 8
- [31] Gensheng Pei, Fumin Shen, Yazhou Yao, Guo-Sen Xie, Zhenmin Tang, and Jinhui Tang. Hierarchical feature alignment network for unsupervised video object segmentation. In *ECCV*. Springer, 2022. 2, 3, 6, 7
- [32] Federico Perazzi, Jordi Pont-Tuset, Brian McWilliams, Luc Van Gool, Markus Gross, and Alexander Sorkine-Hornung. A benchmark dataset and evaluation methodology for video object segmentation. In *CVPR*, 2016. 2, 6
- [33] Andreas Philipp and Daniel Goehring. Analytic collision risk calculation for autonomous vehicle navigation. In *ICRA*. IEEE, 2019. 1
- [34] Chiara Plizzari, Mirco Planamente, Gabriele Goletto, Marco Cannici, Emanuele Gusso, Matteo Matteucci, and Barbara Caputo. E2 (go) motion: Motion augmented event stream for egocentric action recognition. In *CVPR*, 2022. 3
- [35] Jordi Pont-Tuset, Federico Perazzi, Sergi Caelles, Pablo Arbeláez, Alex Sorkine-Hornung, and Luc Van Gool. The 2017 davis challenge on video object segmentation. *arXiv preprint arXiv:1704.00675*, 2017. 2, 5
- [36] Anurag Ranjan, Varun Jampani, Lukas Balles, Kihwan Kim, Deqing Sun, Jonas Wulff, and Michael J Black. Competitive collaboration: Joint unsupervised learning of depth, camera motion, optical flow and motion segmentation. In *CVPR*, 2019. 3
- [37] Sucheng Ren, Wenxi Liu, Yongtuo Liu, Haoxin Chen, Guoqiang Han, and Shengfeng He. Reciprocal transformations for unsupervised video object segmentation. In *CVPR*, 2021. 2, 3, 7
- [38] Shintaro Shiba, Yoshimitsu Aoki, and Guillermo Gallego. Secrets of event-based optical flow. In *ECCV*. Springer, 2022. 3
- [39] Jasdeep Singh, Subrahmanyam Murala, and G Kosuru. Multi domain learning for motion magnification. In *CVPR*, 2023. 8
- [40] Timo Stoffregen, Guillermo Gallego, Tom Drummond, Lindsay Kleeman, and Davide Scaramuzza. Event-based motion segmentation by motion compensation. In *ICCV*, 2019. 2
- [41] Maryam Sultana, Arif Mahmood, and Soon Ki Jung. Unsupervised moving object detection in complex scenes using adversarial regularizations. *IEEE TMM*, 23:2005–2018, 2020. 2
- [42] Deqing Sun, Xiaodong Yang, Ming-Yu Liu, and Jan Kautz. Pwc-net: Cnns for optical flow using pyramid, warping, and cost volume. In *CVPR*, 2018. 1
- [43] Guolei Sun, Yun Liu, Hao Tang, Ajad Chhatkuli, Le Zhang, and Luc . Mining relations among cross-frame affinities for video semantic segmentation. In *ECCV*. Springer, 2022. 2
- [44] Zhaoning Sun, Nico Messikommer, Daniel Gehrig, and Davide Scaramuzza. Ess: Learning event-based semantic segmentation from still images. In *ECCV*. Springer, 2022. 3, 6
- [45] Kevin Ta, David Bruggemann, Tim Brödermann, Christos Sakaridis, and Luc Van Gool. L2e: Lasers to events for 6-dof extrinsic calibration of lidars and event cameras. In *ICRA*. IEEE, 2023. 3
- [46] Matthew Tancik, Vincent Casser, Xinchun Yan, Sabeek Pradhan, Ben Mildenhall, Pratul P Srinivasan, Jonathan T Barron, and Henrik Kretzschmar. Block-nerf: Scalable large scene neural view synthesis. In *CVPR*, 2022. 1
- [47] Zachary Teed and Jia Deng. Raft: Recurrent all-pairs field transforms for optical flow. In *ECCV*. Springer, 2020. 1, 5
- [48] Pavel Tokmakov, Karteek Alahari, and Cordelia Schmid. Learning motion patterns in videos. In *CVPR*, 2017. 2
- [49] Pavel Tokmakov, Cordelia Schmid, and Karteek Alahari. Learning to segment moving objects. *IJCV*, 127:282–301, 2019. 2
- [50] Abhishek Tomy, Anshul Paigwar, Khushdeep S Mann, Alessandro Renzaglia, and Christian Laugier. Fusing event-based and rgb camera for robust object detection in adverse conditions. In *ICRA*. IEEE, 2022. 2, 3, 4, 8
- [51] Yi-Hsuan Tsai, Ming-Hsuan Yang, and Michael J Black. Video segmentation via object flow. In *CVPR*, 2016. 8
- [52] Ashish Vaswani, Noam Shazeer, Niki Parmar, Jakob Uszkoreit, Llion Jones, Aidan N Gomez, Łukasz Kaiser, and Illia Polosukhin. Attention is all you need. *NeurIPS*, 30, 2017. 2
- [53] Wenguan Wang, Hongmei Song, Shuyang Zhao, Jianbing Shen, Sanyuan Zhao, Steven CH Hoi, and Haibin Ling. Learning unsupervised video object segmentation through visual attention. In *CVPR*, 2019. 2, 3
- [54] Yue Wu, Rongrong Gao, Jaesik Park, and Qifeng Chen. Future video synthesis with object motion prediction. In *CVPR*, 2020. 1
- [55] Ruihao Xia, Chaoqiang Zhao, Meng Zheng, Ziyang Wu, Qiyu Sun, and Yang Tang. Cmda: Cross-modality domain adaptation for nighttime semantic segmentation. In *ICCV*, 2023. 6
- [56] Christopher Xie, Yu Xiang, Zaid Harchaoui, and Dieter Fox. Object discovery in videos as foreground motion clustering. In *CVPR*, 2019. 2
- [57] Junyu Xie, Weidi Xie, and Andrew Zisserman. Segmenting moving objects via an object-centric layered representation. *NeurIPS*, 2022. 1
- [58] Rui Xu, Xiaoxiao Li, Bolei Zhou, and Chen Change Loy. Deep flow-guided video inpainting. In *CVPR*, 2019. 1
- [59] Shu Yang, Lu Zhang, Jinqing Qi, Huchuan Lu, Shuo Wang, and Xiaoxing Zhang. Learning motion-appearance co-attention for zero-shot video object segmentation. In *ICCV*, 2021. 2, 3, 7
- [60] Yanchao Yang, Antonio Loquercio, Davide Scaramuzza, and Stefano Soatto. Unsupervised moving object detection via contextual information separation. In *CVPR*, 2019. 2

- [61] Yanchao Yang, Brian Lai, and Stefano Soatto. Dystab: Unsupervised object segmentation via dynamic-static bootstrapping. In *CVPR*, 2021. 2
- [62] Zongxin Yang, Yunchao Wei, and Yi Yang. Associating objects with transformers for video object segmentation. *NeurIPS*, 34:2491–2502, 2021. 1
- [63] Yichen Yuan, Yifan Wang, Lijun Wang, Xiaoqi Zhao, Huchuan Lu, Yu Wang, Weibo Su, and Lei Zhang. Isomer: Isomeric transformer for zero-shot video object segmentation. In *ICCV*, 2023. 1, 2, 3, 6, 7
- [64] Jiaming Zhang, Kailun Yang, and Rainer Stiefelham. Is-safe: Improving semantic segmentation in accidents by fusing event-based data. In *IROS*. IEEE, 2021. 6
- [65] Kaihua Zhang, Zicheng Zhao, Dong Liu, Qingshan Liu, and Bo Liu. Deep transport network for unsupervised video object segmentation. In *ICCV*, 2021. 2
- [66] Shaobo Zhang, Lei Sun, and Kaiwei Wang. A multi-scale recurrent framework for motion segmentation with event camera. *IEEE Access*, 2023. 3
- [67] Mingmin Zhen, Shiwei Li, Lei Zhou, Jiayang Shang, Haoan Feng, Tian Fang, and Long Quan. Learning discriminative feature with crf for unsupervised video object segmentation. In *ECCV*. Springer, 2020. 3
- [68] Tianfei Zhou, Shunzhou Wang, Yi Zhou, Yazhou Yao, Jianwu Li, and Ling Shao. Motion-attentive transition for zero-shot video object segmentation. In *AAAI*, 2020. 2
- [69] Tianfei Zhou, Fatih Porikli, David J Crandall, Luc Van Gool, and Wenguan Wang. A survey on deep learning technique for video segmentation. *IEEE TPAMI*, 45(6):7099–7122, 2022. 2
- [70] Yi Zhou, Guillermo Gallego, Xiuyuan Lu, Siqi Liu, and Shaojie Shen. Event-based motion segmentation with spatio-temporal graph cuts. *IEEE TNNLS*, 2021. 3
- [71] Yifeng Zhou, Xing Xu, Fumin Shen, Xiaofeng Zhu, and Heng Tao Shen. Flow-edge guided unsupervised video object segmentation. *IEEE TCSVT*, 32(12):8116–8127, 2021. 2
- [72] Zhuyun Zhou, Zongwei Wu, Rémi Boutteau, Fan Yang, Cédric Demonceaux, and Dominique Ginjac. Rgb-event fusion for moving object detection in autonomous driving. In *ICRA*. IEEE, 2023. 2, 5, 6
- [73] Alex Zihao Zhu, Dinesh Thakur, Tolga Özaslan, Bernd Pfrommer, Vijay Kumar, and Kostas Daniilidis. The multi-vehicle stereo event camera dataset: An event camera dataset for 3d perception. *IEEE RAL*, 3(3):2032–2039, 2018. 3
- [74] Yi-Fan Zuo, Jiaqi Yang, Jiaben Chen, Xia Wang, Yifu Wang, and Laurent Kneip. Devo: Depth-event camera visual odometry in challenging conditions. In *ICRA*. IEEE, 2022. 3